Available online at www.sciencedirect.com
SCIENCE DIRECT®
International Journal of Heat and Mass Transfer 48 (2005) 2673–2683
International Journal of HEAT and MASS TRANSFER
www.elsevier.com/locate/ijhmt

Heat transfer enhancement in nano-fluids suspensions: Possible mechanisms and explanations

Johnathan J. Vadasz [a,1], Saneshan Govender [a], Peter Vadasz [b,*]

[a] School of Mechanical Engineering, University of KZ-Natal, King George V Ave., Durban 4001, South Africa
[b] Department of Mechanical Engineering, Northern Arizona University, P.O. Box 15600, Flagstaff, AZ 86011-5600, USA

Received 13 December 2004; received in revised form 31 January 2005
Available online 29 March 2005

Abstract

The spectacular heat transfer enhancement revealed experimentally in nano-fluids suspensions is being investigated theoretically at the macro-scale level aiming at explaining the possible mechanisms that lead to such impressive experimental results. In particular, the possibility that thermal wave effects via hyperbolic heat conduction could have been the source of the excessively improved effective thermal conductivity of the suspension is shown to provide a viable explanation although the investigation of alternative possibilities is needed prior to reaching an ultimate conclusion.

Keywords: Nano-fluids; Nano-particles suspension; Heat transfer enhancement; Effective thermal conductivity

1. Introduction

Heat conduction in fluids at the macro-level is very poor because most affordable fluids have very low thermal conductivity values compared with solids. Crystalline solids have thermal conductivity values of 1–3 orders of magnitude larger than those of fluids [1].

The reported breakthrough in substantially increasing the thermal conductivity of fluids by adding very small amounts of suspended metallic or metallic oxide nano-particles (Cu, CuO, Al_2O_3) to the fluid [1,2], or alternatively using nano-tube suspensions [3,4] is intriguing. The latter is important not only because of the face value of its possibility to direct implementation in technological applications but also because both results clearly conflict with theoretical anticipations based on existing theories and models (see discussion on the conflict between theory and experiments in Choi et al. [3]). These results, if independently confirmed, open two distinct avenues of opportunities: (a) Their direct application to different technologies in improving substantially the operating efficiencies and reducing both operating as well as capital production costs. Better efficiency allows for lower pumping power and less heat transfer area, hence saving in both operating as well as fixed costs. Better efficiency also minimizes the adverse impact that energy-producing technologies have on the environment, i.e. less pollutants per kWatt generated. (b) By discovering the correct mechanism and theory that underlies this phenomenon may extend design options in developing processes and devices that apply these mechanisms, hence opening the door to yet unknown and limitless

* Corresponding author. Tel.: +1 928 523 5843; fax: +1 928 523 8951.
E-mail addresses: vadaszj@ukzn.ac.za (J.J. Vadasz), peter.vadasz@nau.edu (P. Vadasz).
[1] Tel.: +27 31 260 7379; fax: +27 31 260 7002.

0017-9310/$ - see front matter
doi:10.1016/j.ijheatmasstransfer.2005.01.023

Nomenclature

a_*	radius of the platinum wire
c_*	wave speed, equals $\sqrt{\alpha_*/\tau_*}$
d_*	depth of the platinum strip
Fo	Fourier number, equals $\alpha_*\tau_*/L_*^2$
i	electrical current
k_*	effective thermal conductivity of the suspension
l_*	length of the platinum wire/strip
L_*	gap distance between the walls of a slab
$\boldsymbol{q}_*$	heat flux
q_{L^*}	horizontal heat flux on the boundary of the platinum strip, at $x_* = L_*$
$\dot{q}_{l^*}$	rate of heat generated by Joule heating in the platinum wire per unit length of wire
R	electrical resistance, dimensional
r_*	radial variable coordinate
t_*	time
T	dimensionless temperature, equals $(T_*-T_{C^*})k_*/(\mid q_{L^*} \mid L_*)$
T_{C^*}	coldest wall temperature, dimensional
T_{1*}	temperature measured at time t_*1
T_{2*}	temperature measured at time t_*2
V	voltage across the platinum wire/strip, dimensional
x	horizontal variable co-ordinate

Greek symbols

α_*	effective thermal diffusivity of the suspension
τ_*	relaxation time in hyperbolic thermal conduction

Subscripts

*	dimensional values
cr	critical values

possibilities of new processes and devices that use heat transfer.

We have redrawn the results reported by Eastman et al. [1] for a ''suspended nano-particles'' system and we present them in Fig. 1a where two major deductions can be made: (a) The impact of the copper nano-particles (that the authors, Eastman et al. [1] succeeded to keep stable in the suspension due to the particular technique they used to manufacture them) on the effective thermal conductivity of the suspension is unexpectedly high. A very small amount (less than 1% in terms of volume fraction) of copper nano-particles can improve the thermal conductivity of the suspension by 40%. (b) Even metal-oxides at small quantities (4% in terms of volume fraction) can produce a substantial increase of about 20% in the effective thermal conductivity of the suspension.

The experimental results reported by Choi et al. [3] of multiwalled carbon nano-tubes suspended in oil were redrawn and are presented in Fig. 1b. An even more impressive improvement of the effective thermal conductivity is detected. Over 150% improvement of the effective thermal conductivity (a factor of 2.5 higher thermal conductivity) at a volume fraction of 1% is indeed spectacular.

Moreover, Choi et al. [3] compared their results with existing theories, some of them going back to the start of the last century, e.g. [5–11]. The reported experimental results are by one order of magnitude greater than the predictions based on existing theories and models. More recent approaches [12] also cannot explain this discrepancy.

On the other hand, a reduction in the effective thermal conductivity of the nano-particle-host medium is anticipated by existing theories for length scales smaller than the phonon mean free path in the host material [13,14]. There is a clear and appealing need to settle the conflict between the recent experimental results and the theories or models. Possible explanations for the divergence between theory and experiments were suggested and explored very basically by Keblinski et al. [15]. Brownian motion of the particles, molecular-level layering of the liquid at the liquid/particle interface, the nature of heat transport within the nano-particles and effects of nano-particle clustering were investigated. While these investigations were not done in detail but mainly at the very basic level, Keblinski et al. [15] show that the ''*key factors in understanding thermal properties of nano-fluids are the ballistic, rather than diffusive, nature of heat transport in the nano-particles*, combined with direct or fluid mediated clustering effects that provide paths for rapid heat transport''. If this conclusion is correct then the experimental results obtained at the macro-system level reflect the wave effects impact on the macro-system behavior rather than the diffusion mechanism. It implies that Fourier Law (representing the diffusion mechanism) is not valid even at the macro-system level when nano-elements are suspended in the fluid. The immediate conclusion from the latter deduction is that the transient hot wire method (THW) that was used by Eastman et al. [1], Lee et al. [2] and Choi et al. [3] to measure the nano-fluid suspension's effective thermal conductivity is not appropriate because it uses the Fourier Law of heat conduction

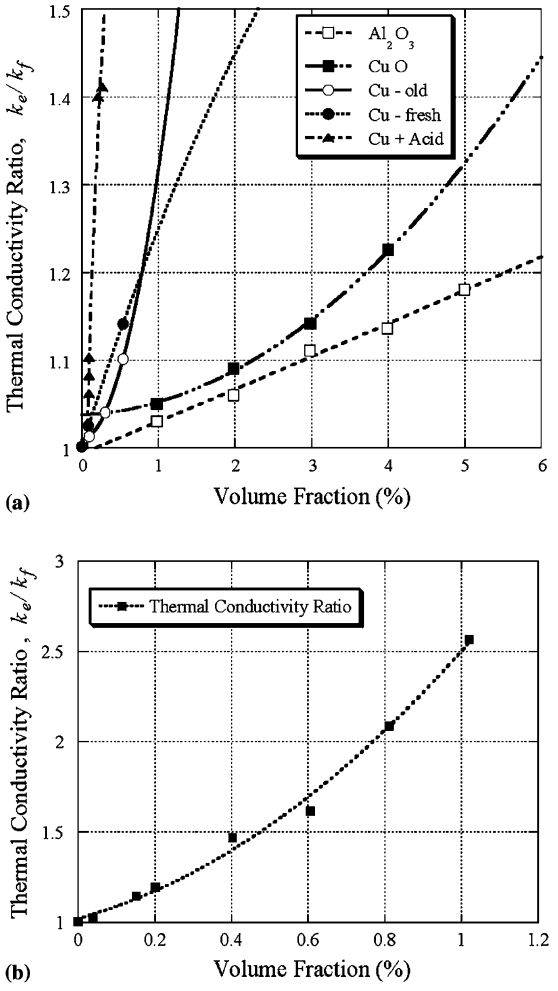

Fig. 1. Thermal conductivity enhancement in systems consisting of (a) nano-particles suspended in ethylene glycol as reported by Eastman et al. [1] and (b) multiwalled carbon nano-tubes suspended in oil, as reported by Choi et al. [3] (here redrawn from published data).

as its fundamental principle for estimating the thermal conductivity [16,17]. Eastman et al. [1] indicate the way the thermal conductivity is being evaluated by using Fourier Law in the transient hot wire method (THW). Therefore, based on this simple logic the excessive values of effective thermal conductivity calculated based on the experimental data might need a correction to account for deviations from Fourier Law. Still the question of why this apparent substantial heat flux enhancement occurred was not yet addressed. The mechanisms suggested by Keblinski et al. (2002) are all possible. However, the way these nano or molecular level mechanisms are being lumped into such an impressive effect at the macro-system level is not yet known, nor proposed by Keblinski et al. [15]. Recent research results presented by Xue et al. [18] eliminate the molecular-level layering of the liquid at the liquid/particle interface as a possible heat transfer enhancement mechanism. The authors [18] conclude that "the experimentally observed large enhancement of thermal conductivity in suspensions of solid nano-size particles (nano-fluids) can not be explained by altered thermal transport properties of the layered liquid". While the reported results are a direct consequence of the presence of nano-elements in the suspension, the measurements were not performed at the nano-scale, but rather at the macro/meso-scale. As a result the interest should be focused not only on what occurs at the nano-scale but rather on how the heat transfer at the macro/meso-scale is substantially affected by a very small presence (less than 1% in volume) of an extremely small concentration of suspended elements (nano-elements).

There are in our view about six possible reasons for the anomalously increased effective thermal conductivity, which can be classified as follows:

(i) Hyperbolic [19–22]) or Dual-phase-lagging [23–26]) thermal wave effects not accounted for in using the THW data processing combined with extremely high values of the time lag τ_* due to the heterogeneous mixture (see [25,26]).
(ii) Thermal resonance due to hyperbolic thermal waves combined with an amplified periodic signal possibly from short-radio-waves or cellular phones (1.9 GHz, 800 MHz frequencies) (see [27]).
(iii) Particle driven, or thermally driven, natural convection.
(iv) Convection induced by electro-phoresis.
(v) Hyperbolic thermal natural convection.
(vi) Any combination of the above.

The first particular possibility that needs exploration is that the nano/molecular level wave effects at the nano-elements' interface make the hyperbolic (wave) heat transfer effects at the macro-level significant. Then, a corresponding correction of converting the experimental data into the effective thermal conductivity results needs to be introduced. The latter forms the objective of the present investigation in terms of introducing the hyperbolic thermal wave corrections based on Cattaneo [19] and Vernotte [20–22] constitutive relationship for heat conduction and checking whether such effects may have been the reason behind the excessive effective thermal conductivity results in nano-fluid suspensions.

2. Experimental methods for thermal conductivity estimation

The transient hot wire (THW) method for estimating experimentally the thermal conductivity of solids [28]

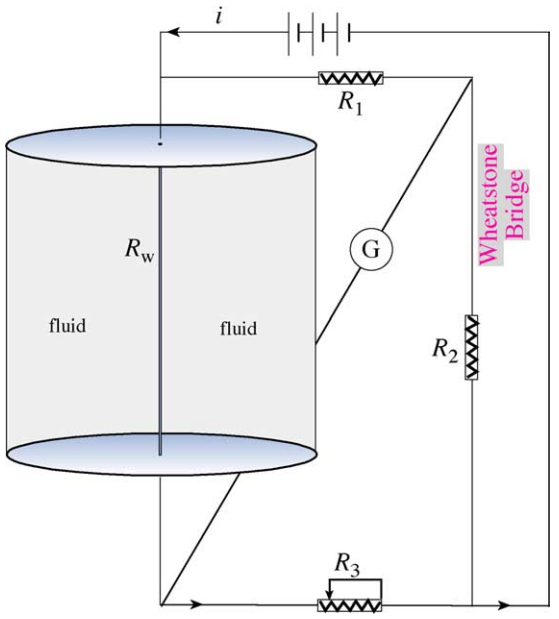

Fig. 2. A Wheatstone bridge used to measure the electrical resistance of the platinum wire/strip as applicable in the transient hot-wire/transient hot-strip methods of estimation of thermal conductivity.

and fluids [29–31] established itself as the most accurate, reliable and robust technique [32]. It replaced the steady state methods primarily because of the difficulty to determine that steady state conditions have indeed been established and for fluids the difficulty in preventing the occurrence of natural convection and consequently the difficulty in eliminating the natural convection effects on the heat flux. The method consists in principle of determining the thermal conductivity of a selected material/fluid by observing the rate at which the temperature of a very thin platinum wire (5–80 μm) increases with time after a step change in voltage has been applied to it. The platinum wire is embedded vertically in the selected material/fluid and serves as a heat source as well as a thermometer, as presented schematically in Fig. 2. The temperature of the platinum wire is established by measuring its electrical resistance, the latter being related to the temperature via a well-known relationship. A Wheatstone bridge is used to measure the electrical resistance R_w of the platinum wire (see Fig. 2). The electrical resistance of the potentiometer R_3 is adjusted until the reading of the galvanometer G shows zero current. When the bridge is balanced as indicated by a zero current reading on the galvanometer G, the value of R_w can be established from the known electrical resistances R_1, R_2 and R_3 by using the balanced Wheatstone bridge relationship $R_w = R_1R_3/R_2$. Because of the very small diameter (micrometer size) and high thermal conductivity of the platinum wire the latter can be regarded as a line source in an otherwise infinite cylindrical medium. The rate of heat generated per unit length (l_*) of platinum wire is therefore $\dot{q}_{l^*} = iV/l_*$ [W/m], where i is the electric current flowing through the wire and V is the voltage drop across the wire. Solving for the radial heat conduction due to this line heat source leads to a temperature solution in the following closed form that can be expanded in an infinite series as follows:

$$T_* = \frac{\dot{q}_{l^*}}{4\pi k_*} Ei\left(\frac{r_*^2}{4\alpha_* t_*}\right) = \frac{\dot{q}_{l^*}}{4\pi k_*}\left[-\gamma + \ln\left(\frac{4\alpha_* t_*}{r_*^2}\right) + \frac{r_*^2}{4\alpha_* t_*} - \frac{r_*^4}{64\alpha_*^2 t_*^2} + \frac{r_*^6}{1152\alpha_*^3 t_*^3} - \cdots\right] \quad (1)$$

where $Ei(\cdot)$ represents the exponential integral function, and $\gamma = \ln(\sigma) = 0.5772156649$ is Euler's constant. For a line heat source embedded in a cylindrical cell of infinite radial extent and filled with the test fluid one can use the approximation $r_*^2/4\alpha_* t_* \ll 1$ in Eq. (1) to truncate the infinite series and yield

$$T_* \approx \frac{\dot{q}_{l^*}}{4\pi k_*}\left[-\gamma + \ln\left(\frac{4\alpha_* t_*}{r_*^2}\right) + O\left(\frac{r_*^2}{4\alpha_* t_*}\right)\right] \quad (2)$$

Eq. (2) reveals a linear relationship, on a logarithmic time scale, between the temperature and time. For $r_* = a_*$, a_* being the radius of the platinum wire, the condition for the series truncation $r_*^2/4\alpha_* t_* \ll 1$ can be expressed in the following equivalent form that provides the validity condition of the approximation in the form

$$t_* \gg \frac{a_*^2}{4\alpha_*} \quad (3)$$

For any two temperature readings T_{1*} and T_{2*} recorded at the times t_{1*} and t_{2*} respectively the temperature difference $(T_{2*} - T_{1*})$ can be approximated by using Eq. (2) in the form

$$(T_{2^*} - T_{1^*}) \approx \frac{iV}{4\pi k_* l_*}\left[\ln\left(\frac{t_{2^*}}{t_{1^*}}\right)\right] \quad (4)$$

where we replaced the heat source with its explicit dependence on the i, V and l_*, i.e. $\dot{q}_{l^*} = iV/l_*$. From Eq. (4) one can express the thermal conductivity k_* explicitly in the form

$$k_* \approx \frac{iV}{4\pi(T_{2^*} - T_{1^*})l_*}\left[\ln\left(\frac{t_{2^*}}{t_{1^*}}\right)\right] \quad (5)$$

Eq. (5) is a very accurate way of estimating the thermal conductivity as long as the validity conditions for appropriateness of the problem derivations used above are fulfilled. A finite length of the platinum wire, the finite size of the cylindrical container, the heat capacity of the platinum wire, and possibly natural convection effects are examples of possible deviations of any realistic system from the one used in deriving Eq. (5). De Groot et al.

[29], Healy et al. [30] and Kestin and Wakeham [31] introduce an assessment of these deviations and possible corrections to the THW readings to improve the accuracy of the results. In general all the deviations indicated above could be eliminated via the proposed corrections provided the validity condition listed in Eq. (3) is enforced as well as an additional condition that ensures that natural convection is absent. The validity condition (3) implies the application of Eq. (5) for long times only. However, when evaluating this condition (3) to data used in the nano-fluids suspensions experiments considered in this paper one obtains explicitly the following values. For a 76.2 μm diameter of platinum wire used by Eastman et al. [1], Lee et al. [2]), Choi et al. [3], the wire radius is $a_* = 3.81 \times 10^{-5}$ m leading to $a_*^2/4\alpha_* = 3.9$ ms for ethylene glycol and $a_*^2/4\alpha_* = 4.2$ ms for oil, producing the explicit validity condition $t_* \gg 3.9$ ms for ethylene glycol and $t_* \gg 4.2$ ms for oil. The long times beyond which the solution (5) can be used reliably are therefore of the order of a tens of milliseconds, not so long in the actual practical sense. On the other hand the experimental time range is limited from above as well in order to ensure the lack of natural convection that develops at longer time scales. Xuan and Li [4] estimate this upper limit for the time that an experiment may last before natural convection develops as about 5 s. They indicate that "An experiment lasts about 5 s. If the time is longer, the temperature difference between the hot-wire and the sample fluid increases and free convection takes place, which may result in errors". Lee et al. [2] while using the THW method and providing experimental data in the time range of 1–10 s, indicate in their Fig. 3 the "*valid range of data reduction*" to be between 3 s and 6 s. Our estimations evaluated above confirm these lower limits as a very safe constraint and we assume that the upper limits listed by Xuan and Li [4] and Lee et al. [2] are also good estimates, leading to the validity condition of the experimental results to be within the following estimated time range of $0.03\text{ s} < t_* < 5\text{ s}$. The valid range for data reduction used by Lee et al. [2], i.e. $3\text{ s} < t_* < 6\text{ s}$ should also be satisfactory. Within this time range the experimental results should produce a linear relationship, on a logarithmic time scale, between the temperature and time.

While the application of the method to solids and gases is straightforward its corresponding application to electrically conducting liquids needs further attention. The experiments conducted in nano-fluids suspensions listed above used a thin electrical insulation coating layer to cover the platinum wire instead of using the bare metallic wire, a technique developed by Nagasaka and Nagashima [33]. The latter is aimed at preventing problems such as electrical current flow through the liquid causing ambiguity of the heat generation in the wire.

A transient hot strip (THS) method using a rectangular geometry was developed as an equivalent alternative to the transient hot wire (THW) method that applies to a cylindrical geometry. The transient hot strip (THS) method uses a very thin metal foil instead of the hot wire to undertake identical functions as presented in a review by Gustafsson [34]. It applies therefore to a rectangular geometry and its accuracy, uncertainty, advantages and disadvantages as compared to the THW method were presented by Hammerschmidt and Sabuga [32].

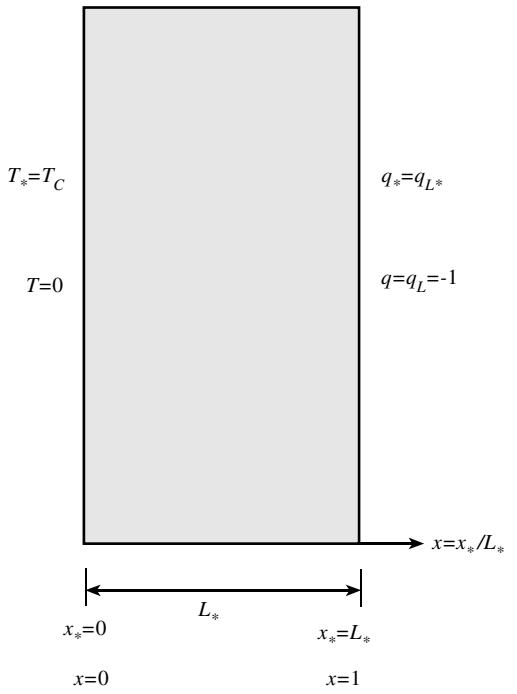

Fig. 3. Problem formulation of the heat conduction in a slab subject to constant heat flux on one wall and constant temperature on the other wall.

3. Problem formulation and thermal wave effects

The present investigation focuses on thermal wave effects via the constitutive model suggested by Cattaneo [19] and Vernotte [20–22] and the possible deviation of the experimental results due to these effects from the expected Fourier conduction. To investigate preliminary the possibility that thermal wave effects might have been the cause of the apparently spectacular enhancement of the effective thermal conductivity of the suspension we consider the thermal conduction in a rectangular geometry due to a plane heat source (see Fig. 3) via the hyperbolic heat conduction formulation as well as via a Fourier heat conduction formulation and compare the two. The rectangular geometry used here applies to a transient hot strip method of evaluation of the thermal conductivity and the comparison applies to deviations

between Fourier to hyperbolic thermal conduction as applicable to the THS method and the required corrections in accounting for the latter deviations.

Consider the slab as described in Fig. 3 subject to a constant heat flux on its right wall q_{L^*}, representing the heat flux from the hot strip to the fluid due to the uniform Joule heating generated in the thin hot strip by the electric current, and a constant cold temperature T_C on the left wall. The hyperbolic conduction phenomenon is governed by the constitutive relationship between the heat flux and temperature gradient in the form

$$\tau_* \frac{\partial \boldsymbol{q}_*}{\partial t_*} + \boldsymbol{q}_* = -k_* \nabla_* T_* \tag{6}$$

where τ_* is the relaxation time and α_* is the thermal diffusivity, leading to the hyperbolic heat conduction equation

$$\frac{1}{c_*^2}\frac{\partial^2 T_*}{\partial t_*^2} + \frac{1}{\alpha_*}\frac{\partial T_*}{\partial t_*} = \nabla_*^2 T_* \tag{7}$$

where $c_* = \sqrt{\alpha_*/\tau_*}$ is the wave speed. Eqs. (6) and (7) may be transferred into a dimensionless form by introducing the following scales L_*, L_*^2/α_*, $|q_{L^*}|$, $|q_{L^*}| L_*/k_*$ for the space variable, time variable, heat flux and temperature difference, respectively. This leads to the following definitions of the dimensionless variables

$$x = \frac{x_*}{L_*}, \quad t = \frac{\alpha_* t_*}{L_*^2}, \quad q = \frac{q_*}{|q_{L^*}|}, \quad T = \frac{(T_* - T_{C^*})k_*}{|q_{L^*}| L_*} \tag{8}$$

that transform Eqs. (6) and (7) into their corresponding dimensionless form

$$Fo\frac{\partial \boldsymbol{q}}{\partial t} + \boldsymbol{q} = -k\nabla T \tag{9}$$

$$Fo\frac{\partial^2 T}{\partial t^2} + \frac{\partial T}{\partial t} = \nabla^2 T \tag{10}$$

where $Fo = \alpha_* \tau_* / L_*^2$ is the Fourier number. For the one-dimensional slab considered here Eqs. (9) and (10) take the form

$$Fo\frac{\partial \boldsymbol{q}}{\partial t} + \boldsymbol{q} = -k\frac{\partial T}{\partial x} \tag{11}$$

$$Fo\frac{\partial^2 T}{\partial t^2} + \frac{\partial T}{\partial t} = \frac{\partial^2 T}{\partial x^2} \tag{12}$$

The analysis and investigation of Eq. (12) was extensively covered in excellent papers and reviews, such as Özisik and Tzou [35], Haji-Sheikh et al. [36], Wang [37], Frankel et al. [38], and Vick and Özisik [39], to name only a few. The solution to Eq. (12) subject to the boundary and initial conditions considered in this paper that are expressed in the following dimensionless form

$$\begin{aligned} &x = 0 : T = 0 \\ &x = 1 : q_L = -1 \rightarrow (\partial T/\partial x)_{x=1} = 1 \end{aligned} \tag{13}$$

$$t = 0 : \begin{cases} T = T_0 = \text{const.} \\ \dot{T} = \dot{T}_0 = \text{const.} \end{cases} \tag{14}$$

is expressed in terms of orthogonal eigenfunctions in the form

$$\begin{aligned} T = x &+ e^{\lambda_c t}\sum_{n=0}^{M_0}\left[A_n e^{\lambda_{1sn} t} + B_n e^{\lambda_{2sn} t}\right]\sin\left[\frac{(2n+1)\pi}{2}x\right] \\ &+ \left[A_{n,\mathrm{cr}} + B_{n,\mathrm{cr}} t\right]e^{\lambda_c t}\sin\left[\frac{(2n_{\mathrm{cr}}+1)\pi}{2}x\right]\delta_{n_{\mathrm{cr}},j} \\ &+ e^{\lambda_c t}\sum_{n=M_1}^{\infty}\left\{\frac{A_n}{2}\left[\cos\left(\frac{(2n+1)\pi}{2}x - \lambda_{in} t\right)\right.\right. \\ &\left.\left. - \cos\left(\frac{(2n+1)\pi}{2}x + \lambda_{in} t\right)\right] \right. \\ &+ \frac{B_n}{2}\left[\sin\left(\frac{(2n+1)\pi}{2}x - \lambda_{in} t\right)\right. \\ &\left.\left.\left. + \sin\left(\frac{(2n+1)\pi}{2}x + \lambda_{in} t\right)\right]\right\} \end{aligned} \tag{15}$$

where

$$\lambda_{1n} = \lambda_c + \lambda_{1sn}; \quad \lambda_{2n} = \lambda_c + \lambda_{2sn};$$
$$\lambda_c = -\frac{1}{2Fo} \qquad \forall n < n_{\mathrm{cr}} \tag{16a}$$

$$\lambda_{1n,\mathrm{cr}} = \lambda_{2n,\mathrm{cr}} = \lambda_c = -\frac{1}{2Fo} \quad \forall n = n_{\mathrm{cr}} \tag{16b}$$

$$\lambda_{1n} = \lambda_c + i\lambda_{in}; \quad \lambda_{2n} = \lambda_c - i\lambda_{in};$$
$$\lambda_c = -\frac{1}{2Fo} \qquad \forall n > n_{\mathrm{cr}} \tag{16c}$$

and where we introduced the notation

$$\begin{aligned} &\lambda_{1sn} = -\frac{1}{2Fo}\sqrt{1 - (2n+1)^2\pi^2 Fo}; \\ &\lambda_{2sn} = \frac{1}{2Fo}\sqrt{1 - (2n+1)^2\pi^2 Fo} \qquad \forall n < n_{\mathrm{cr}} \end{aligned} \tag{17a}$$

$$\Delta\lambda = \frac{1}{Fo}\sqrt{1 - (2n+1)^2\pi^2 Fo} \qquad \forall n < n_{\mathrm{cr}} \tag{17b}$$

$$\lambda_{in} = \frac{1}{2Fo}\sqrt{(2n+1)^2\pi^2 Fo - 1} \quad \forall n > n_{\mathrm{cr}} \tag{17c}$$

while the critical value of n, i.e. n_{cr}, was evaluated and can be expressed in the form

$$n_{\mathrm{cr}} = \frac{1}{2}\left(\frac{1}{\pi\sqrt{Fo}} - 1\right) \tag{18}$$

For initial conditions consistent with an initial permanent constant temperature identical to that of the environment, i.e. to T_{C^*}, the dimensionless values of the initial conditions are $T_0 = 0$, $\dot{T}_0 = 0$, leading to the following expressions for the coefficients in the series (15)

$$A_n = \frac{2\lambda_{2n} I_{1n}}{\Delta\lambda}; \quad B_n = -\frac{2\lambda_{1n} I_{1n}}{\Delta\lambda} \qquad \forall n < n_{\rm cr} \tag{19a}$$

$$A_{n,\rm cr} = 2I_{1n,\rm cr}; \quad B_n = -2\lambda_c I_{1n,\rm cr} \qquad \forall n = n_{\rm cr} \tag{19b}$$

$$A_n = -\frac{2\lambda_c}{\lambda_{in}} I_{1n}; \quad B_n = 2I_{1n} \qquad \forall n > n_{\rm cr} \tag{19c}$$

where $I_{1n} = -4(-1)^n/(2n+1)^2\pi^2$. The infinite series in Eq. (15) consists of three separate contributions dictated by the values of M_0 and M_1 defined by

$$M_0 = \lfloor n_{\rm cr} \rfloor - \delta_{n_{\rm cr},j} = \begin{cases} (n_{\rm cr} - 1) & \forall n_{\rm cr} = j,\ j = 0,1,2,3,\ldots \\ \lfloor n_{\rm cr} \rfloor & \forall n_{\rm cr} \neq j,\ j = 0,1,2,3,\ldots \end{cases} \tag{20}$$

$$M_1 = \lfloor n_{\rm cr} \rfloor + 1 = \begin{cases} (n_{\rm cr} + 1) & \forall n_{\rm cr} = j,\ j = 0,1,2,3,\ldots \\ (M_0 + 1) & \forall n_{\rm cr} \neq j,\ j = 0,1,2,3,\ldots \end{cases} \tag{21}$$

where $\delta_{n_{\rm cr},j}$ is the Kronecker delta function defined in the form

$$\delta_{n_{\rm cr},j} = \begin{cases} 1 & \forall n_{\rm cr} = j, j = 0,1,2,3,\ldots \\ 0 & \forall n_{\rm cr} \neq j, j = 0,1,2,3,\ldots \end{cases} \tag{22}$$

and $\lfloor n_{\rm cr} \rfloor$ is the *inclusive floor function* representing the largest integer less than or equal to $n_{\rm cr}$. Therefore M_0 is the *exclusive floor function* representing the largest integer less than $n_{\rm cr}$. The first contribution is a finite series for the terms corresponding to values of $0 < n < n_{\rm cr}$. When $n_{\rm cr} = 0$ corresponding to $Fo = 1/\pi^2$ this contribution is absent. The second contribution is the critical term which is present only if $n_{\rm cr}$ is a non-negative integer. This critical term is absent when $n_{\rm cr}$ is not a non-negative integer, or if $Fo > 1/\pi^2$. The third contribution is an infinite series representing traveling waves that formed via a cascade of frequencies over a wide range of scales. This contribution is present at all times however it may become significantly small if $n_{\rm cr} \gg 1$.

Our primary interest is the temperature value at $x = 1$, or dimensionally at $x_* = L_*$, i.e. T_L. The latter is obtained by substituting $x = 1$ into the solution (15) leading to

$$T_L = 1 + e^{\lambda_c t}\left[\sum_{n=0}^{M_0}(a_n e^{\lambda_{1sn} t} + b_n e^{\lambda_{2sn} t}) + (a_{n,\rm cr} + b_{n,\rm cr} t)\delta_{n_{\rm cr},j} + \sum_{n=M_1}^{\infty}[a_n \sin(\lambda_{in} t) + b_n \cos(\lambda_{in} t)]\right] \tag{23}$$

where the coefficients are defined as follows

$$a_n = (-1)^n A_n = \frac{-8\lambda_{2n}}{(2n+1)^2\pi^2\Delta\lambda}; \quad b_n = (-1)^n B_n = \frac{8\lambda_{1n}}{(2n+1)^2\pi^2\Delta\lambda} \qquad \forall n < n_{\rm cr} \tag{24a}$$

$$a_{n,\rm cr} = (-1)^{n_{\rm cr}} A_{n,\rm cr} = \frac{-8}{(2n+1)^2\pi^2}; \quad b_{n,\rm cr} = (-1)^{n_{\rm cr}} B_{n,\rm cr} = \frac{8\lambda_c}{(2n+1)^2\pi^2} \qquad \forall n = n_{\rm cr} \tag{24b}$$

$$a_n = (-1)^n A_n = \frac{8\lambda_c}{(2n+1)^2\pi^2\lambda_{in}}; \quad b_n = (-1)^n B_n = \frac{-8}{(2n+1)^2\pi^2} \qquad \forall n > n_{\rm cr} \tag{24c}$$

Therefore the temperature $T_L(t)$ at $x = 1$, or dimensionally at $x_* = L_*$, can be presented following Eq. (23) in the following form

$$T_L(t) = \frac{[T_{L^*}(t) - T_{C^*}]k_*}{\mid q_{L^*} \mid L_*} = 1 + h(t) \tag{25}$$

where

$$h(t) = e^{\lambda_c t}\left[\sum_{n=0}^{M_0}(a_n e^{\lambda_{1sn} t} + b_n e^{\lambda_{2sn} t}) + (a_{n,\rm cr} + b_{n,\rm cr} t)\delta_{n_{\rm cr},j} + \sum_{n=M_1}^{\infty}[a_n \sin(\lambda_{in} t) + b_n \cos(\lambda_{in} t)]\right] \tag{26}$$

which produces the following dimensional solution

$$[T_{L^*}(t) - T_{C^*}] = \frac{\mid q_{L^*} \mid L_*}{k_*}[1 + h(t)] \tag{27}$$

4. Analytical estimation of corrections to experimental data

In order to derive the deviations from the Fourier to the hyperbolic thermal conduction solutions and evaluate the required corrections we present the corresponding Fourier solution to the same problem of the slab presented in Fig. 3 subject to a constant heat flux on its right wall q_{L^*}, representing the heat flux to the fluid due to the uniform Joule heating generated in the thin hot strip by the electric current, and a constant cold temperature T_{C^*} on the left wall. The Fourier solution is presented also in terms of orthogonal eigen functions in the form

$$T = x + \sum_{n=0}^{\infty} A_n \exp\left[-\frac{(2n+1)^2\pi^2}{4} t\right] \sin\left[\frac{(2n+1)\pi}{2} x\right] \tag{28}$$

leading to the following solution for the temperature $T_L(t)$ at $x = 1$,

$$[T_{L^*}(t) - T_{C^*}] = \frac{\mid q_{L^*} \mid L_*}{k_*}[1 + f(t)] \tag{29}$$

where

$$f(t) = \sum_{n=0}^{\infty}(-1)^n A_n \exp\left[-\frac{(2n+1)^2\pi^2}{4} t\right] \tag{30}$$

and for initial conditions of $T_0 = 0$ the values of A_n are evaluated and expressed in the form

$$(-1)^n A_n = -\frac{8}{(2n+1)^2\pi^2} \tag{31}$$

which following substitution into Eq. (30) yields

$$f(t) = \sum_{n=0}^{\infty} -\frac{8}{(2n+1)^2\pi^2} \exp\left[-\frac{(2n+1)^2\pi^2}{4}t\right] \tag{32}$$

When evaluating the thermal conductivity by applying the transient hot strip method and using the Fourier Law one obtains from Eq. (29)

$$k_* = \frac{\mid q_{L^*} \mid L_*}{[T_{L^*}(t) - T_{C^*}]}[1 + f(t)] \tag{33}$$

where the temperature difference $[T_{L^*}(t) - T_{C^*}]$ is represented by the recorded experimental data and the value of the wall heat flux $|q_L|$ is evaluated from the Joule heating of the hot strip in the form $\mid q_L \mid = iV/A_{*_{\text{strip}}}$, where $A_{*_{\text{strip}}} = d_* l_*$ is the heat transfer area of the hot strip, with l_* being the length of the strip and d_* the depth of the hot strip.

We apply now a method of *synthetic experimental emulation data* (SEED) to evaluate the deviation between Fourier and hyperbolic thermal conduction. According to the SEED method we assume that the data expressed by $[T_{L^*}(t) - T_{C^*}]$ represent a different than Fourier conduction solution, in this case a hyperbolic thermal conduction solution. Then we substitute in Eq. (33) the values of $[T_{L^*}(t) - T_{C^*}]$ obtained from the hyperbolic solution expressed by Eqs. (27) and (26) to yield

$$\frac{k_{\text{app}}}{k_{\text{act}}} = \frac{[1 + f(t)]}{[1 + h(t)]} \tag{34}$$

where k_{app} is the apparent thermal conductivity obtained from the Fourier conduction solution while k_{act} is the actual thermal conductivity that corresponds to data that follow the hyperbolic conduction, and where $f(t)$ can be evaluated from Eq. (32) while $h(t)$ is evaluated from Eq. (26). The ratio between the two will provide the deviation of the apparent thermal conductivity from the actual one.

5. Results and discussion

Despite the fact that the present paper focuses on transient hot strip results because of the rectangular geometry used we attempted to select dimensional values that are of the same equivalent values as the ones used in the experimental setup of Eastman et al. [1], Lee et al. [2] for metals and metal-oxides suspended in ethylene glycol, or alternatively for nano-tube suspensions in oil used by Choi et al. [3]. Eq. (34) can be evaluated as a function of time for any given value of Fourier number, *Fo*. The dependence of the results on the Fourier number is established due to the dependence of the hyperbolic eigenvalues on *Fo* which are needed in the evaluation of $h(t)$. Other than that the thermal conductivity ratio depends only on the dimensionless time. To convert the latter and express it in terms of the dimensional values of time we use the scaling definition introduced by Eq. (8) in the form $t_* = (L_*^2/\alpha_*)t$. We use a value of $L_* = 0.025$ m which is equivalent to the radius of the cylindrical container used by Eastman et al. [1], Lee et al. [2] and Choi et al. [3], and two different values of thermal diffusivity α_* corresponding to ethylene glycol and oil, respectively, i.e. for ethylene glycol $\alpha_{\text{eg}^*} = 0.939 \times 10^{-7}$ m^2/s while for oil $\alpha_{\text{oil}^*} = 0.87 \times 10^{-7}$ m^2/s. Consequently the time conversion from dimensionless to dimensional follows the following factoring $t_* = 6.656 \times 10^3 t$ s for ethylene glycol, and $t_* = 7.184 \times 10^3 t$ s for oil.

The evaluated dimensionless wall temperature at $x_* = L_*$ which represents the hot-wire/strip temperature was evaluated for data corresponding to ethylene glycol and a Fourier number of $Fo = 0.001$ following both the Fourier as well as the hyperbolic solutions presented by Eqs. (29) and (25), respectively. The results are presented in Fig. 4(a) on a logarithmic time scale and within the time range of between 3 s and 6 s, the latter being identified by Lee et al. [2] as the "valid range for data reduction". From Fig. 4(a) it is evident that within this time range both Fourier as well as the hyperbolic wall temperature solutions are approximately linear in time on a logarithmic time scale. Therefore this linearity cannot confirm the validity of either one of the models as the correct one. The results of the ratio between the "apparent" and "actual" thermal conductivities corresponding to data of ethylene glycol and a Fourier number of $Fo = 0.001$ are presented in Fig. 4(b) where two slightly different time ranges are identified. The experimental time frame used by Lee et al. [2] of $3\text{ s} < t_* < 6$ s reveals that the thermal conductivity ratio varies between $k_{\text{app}}/k_{\text{act}} = 1.46$ and $k_{\text{app}}/k_{\text{act}} = 1.85$. Our own estimation of the valid experimental time frame that is consistent with Xuan and Li [4] as well as with Healy et al. [30] corresponds to $100\text{ ms} < t_* < 5$ s. Within this time frame the thermal conductivity ratio varies between $k_{\text{app}}/k_{\text{act}} = 1.55$ and substantially higher than $k_{\text{app}}/k_{\text{act}} = 5$. To investigate the effect of a small Fourier number we evaluated the thermal conductivity ratio of ethylene glycol for $Fo = 10^{-4}$ and the results are presented in Fig. 5. For an experimental time frame of $100\text{ ms} < t_* < 5$ s. Fig. 5 reveals a variation of the thermal conductivity ratio between $k_{\text{app}}/k_{\text{act}} = 1.04$ and substantially higher than $k_{\text{app}}/k_{\text{act}} = 1.8$. A larger value of Fourier number, i.e. $Fo = 0.01$, with ethylene glycol leads to the results presented in Fig. 6 identifying a variation of the thermal

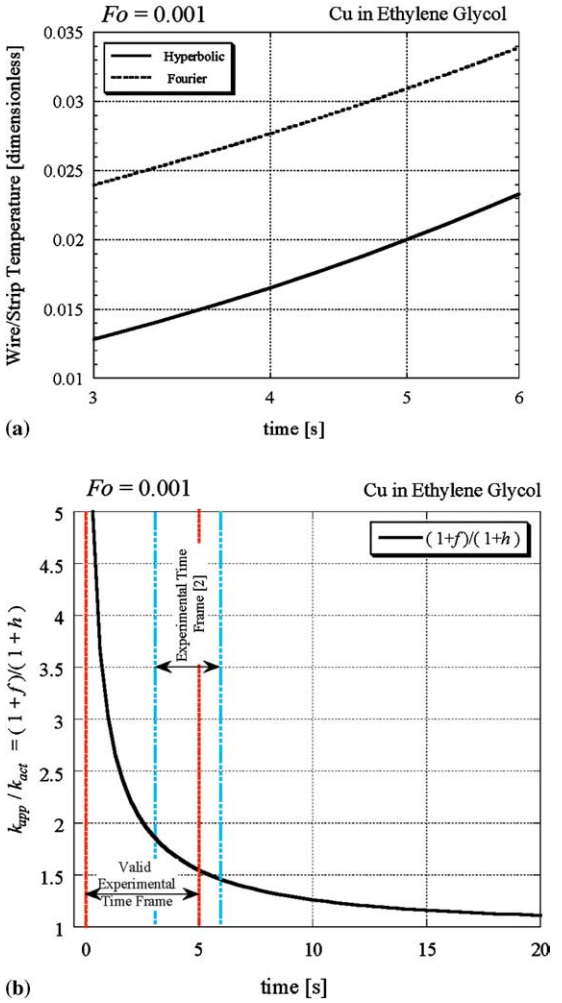

Fig. 4. Comparison between the Fourier and hyperbolic solutions corresponding to properties of ethylene glycol and a Fourier number of $Fo = 0.001$. (a) Hot strip dimensionless temperature within the time range 3 s < t_* < 6 s and (b) thermal conductivity ratio (k_{app}/k_{act}).

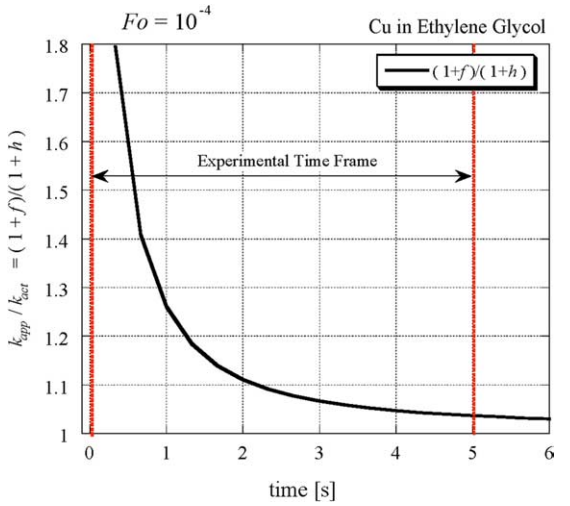

Fig. 5. Thermal conductivity ratio (k_{app}/k_{act}) from the Fourier and hyperbolic solutions corresponding to properties of ethylene glycol and a Fourier number of $Fo = 10^{-4}$.

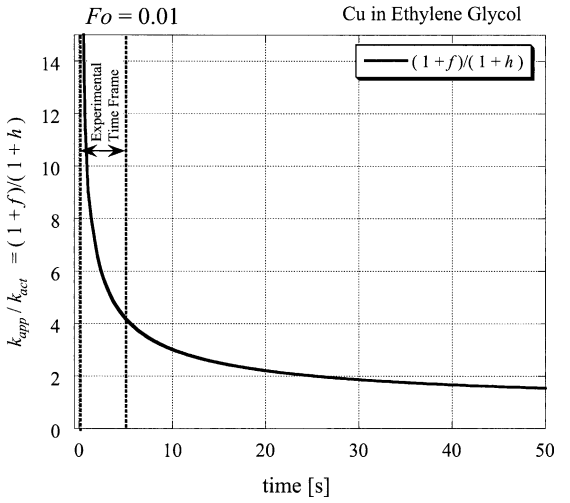

Fig. 6. Thermal conductivity ratio (k_{app}/k_{act}) from the Fourier and hyperbolic solutions corresponding to properties of ethylene glycol and a Fourier number of $Fo = 0.01$.

conductivity ratio between $k_{app}/k_{act} = 4.1$ and substantially higher than $k_{app}/k_{act} = 14$. Similar results corresponding to properties of oil such as the carbon nano-tubes suspensions in oil used by Choi et al. [3] are presented in Figs. 7–9. The results presented in Fig. 7 corresponding to $Fo = 0.001$ show a thermal conductivity ratio variation of between $k_{app}/k_{act} = 1.59$ and substantially beyond $k_{app}/k_{act} = 5$. For a smaller Fourier number, i.e. $Fo = 10^{-4}$ presented in Fig. 8, the variation of the thermal conductivity ratio lies between $k_{app}/k_{act} = 1.04$ and way beyond $k_{app}/k_{act} = 1.8$. Finally Fig. 9 presents results consistent with $Fo = 0.01$ identifying a thermal conductivity ratio variation of between $k_{app}/k_{act} = 4.3$ and far beyond $k_{app}/k_{act} = 14$.

To summarize, the computed analytical results show that the apparent thermal conductivity evaluated via the Fourier conduction constitutive relationship could indeed produce results that show substantial apparent enhancement of the effective thermal conductivity of the nano-fluid suspension if the actual conduction process is governed by a hyperbolic thermal conduction process.

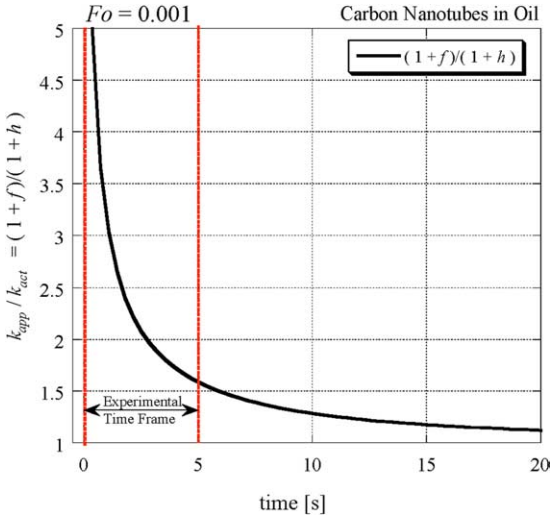

Fig. 7. Thermal conductivity ratio (k_{app}/k_{act}) from the Fourier and hyperbolic solutions corresponding to properties of oil and a Fourier number of $Fo = 0.001$.

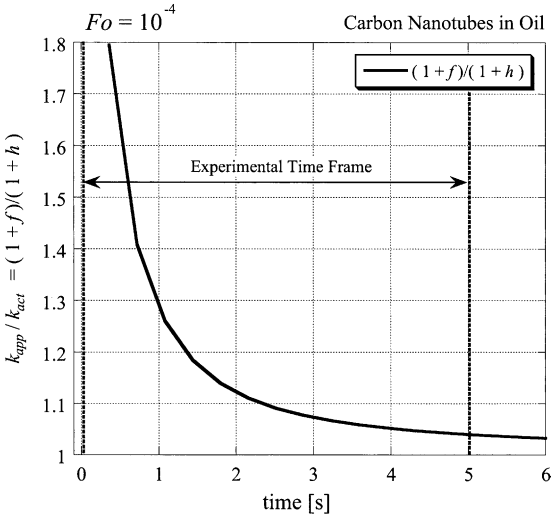

Fig. 8. Thermal conductivity ratio (k_{app}/k_{act}) from the Fourier and hyperbolic solutions corresponding to properties of oil and a Fourier number of $Fo = 10^{-4}$.

6. Conclusions

The impressive heat transfer enhancement revealed experimentally in nano-fluids suspensions was investigated theoretically by applying the hyperbolic heat conduction constitutive relationship and comparing it to the corresponding Fourier conduction results. It is demonstrated that hyperbolic heat conduction could have been the source of the excessively high effective thermal conductivity of the suspension and therefore providing a viable explanation of the anomalous thermal conductivity enhancement. Nevertheless, the investigation of alternative possibilities is needed prior to reaching an ultimate conclusion.

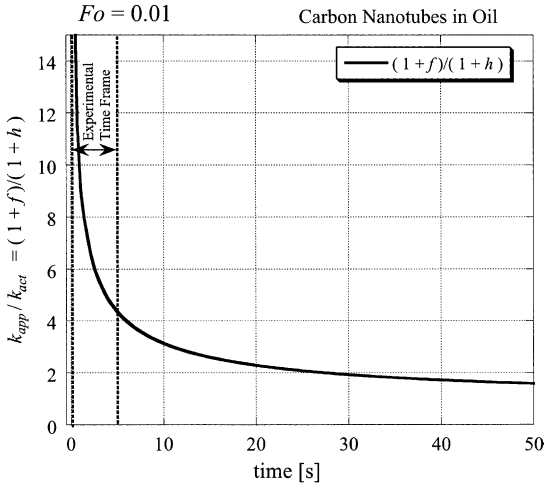

Fig. 9. Thermal conductivity ratio (k_{app}/k_{act}) from the Fourier and hyperbolic solutions corresponding to properties of oil and a Fourier number of $Fo = 0.01$.

Acknowledgment

The authors wish to thank the National Research Foundation (NRF) and the University of KZ-Natal, South Africa, for partially supporting this study.

References

[1] J.A. Eastman, S.U.S. Choi, S. Li, W. Yu, L.J. Thompson, Anomalously increased effective thermal conductivities of ethylene glycol-based nanofluids containing copper nanoparticles, Appl. Phys. Lett. 78 (6) (2001) 718–720.
[2] S. Lee, S.U.-S. Choi, S. Li, J.A. Eastman, Measuring thermal conductivity of fluids containing oxide nanoparticles, ASME J. Heat Transfer 121 (1999) 280–289.
[3] S.U.S. Choi, Z.G. Zhang, W. Yu, F.E. Lockwood, E.A. Grulke, Anomalous thermal conductivity enhancement in nanotube suspensions, Appl. Phys. Lett. 79 (14) (2001) 2252–2254.
[4] Y. Xuan, Q. Li, Heat transfer enhancement of nanofluids, Int. J. Heat Mass Transfer 21 (2000) 58–64.
[5] J.C. Maxwell, A Treatise on Electricity and Magnetism, 3rd edition, Clarendon Press, 1954 reprint, Dover, New York, 1891, pp. 435–441.
[6] R.L. Hamilton, O.K. Crosser, Thermal conductivity of heterogeneous two-component systems, I&EC Fund. 1 (1962) 187–191.
[7] D.J. Jeffrey, Conduction through a random suspension of spheres, Proc. Royal Soc. Lond. A 335 (1973) 355–367.

[8] R.H. Davis, The effective thermal conductivity of a composite material with spherical inclusions, Int. J. Thermophys. 7 (1986) 609–620.
[9] S. Lu, H. Lin, Effective conductivity of composites containing aligned spheroidal inclusions of finite conductivity, J. Appl. Phys. 79 (1996) 6761–6769.
[10] R.T. Bonnecaze, J.F. Brady, A method for determining the effective conductivity of dispersions of particles, Proc. Royal Soc. Lond. A 430 (1990) 285–313.
[11] R.T. Bonnecaze, J.F. Brady, The effective conductivity of random suspensions of spherical particles, Proc. Royal Soc. Lond. A 432 (1991) 445–465.
[12] B.X. Wang, L.P. Zhou, X.F. Peng, A fractal model for predicting the effective thermal conductivity of liquid with suspension of nanoparticles, Int. J. Heat Mass Transfer 46 (2003) 2655–2672.
[13] G. Chen, Nanolocal and nonequilibrium heat conduction in the vicinity of nanoparticles, J. Heat Transfer 118 (1996) 539–545.
[14] G. Chen, Particularities of heat conduction in nanostructures, J. Nanoparticle Res. 2 (2000) 199–204.
[15] P. Keblinski, S.R. Phillpot, S.U.S. Choi, J.A. Eastman, Mechanisms of heat flow in suspensions of nano-sized particles (nanofluids), Int. J. Heat Mass Transfer 45 (2002) 855–863.
[16] J. Kestin, W.A. Wakeham, A contribution to the theory of the transient hot-wire technique for thermal conductivity measurements, Physica 92A (1978) 102–116.
[17] R.A. Perkins, M.L.V. Ramires, C.A. Nieto de Castro, Thermal conductivity of saturated liquid toluene by use of anodized tantalum hot wires at high temperatures, J. Res. Natl. Inst. Standards Technol. 105 (2000) 255–265.
[18] L. Xue, P. Keblinski, S.R. Phillpot, S.U.-S. Choi, J.A. Eastman, Effect of fluid layering at the liquid-solid interface on thermal transport, Int. J. Heat Mass Transfer 47 (2004) 4277–4284.
[19] M.C. Cattaneo, Sur une forme de l'equation de la chaleur eliminant le paradoxe d'une propagation instantanee, Comptes Rendus Hebd. Seances Acad. Sci. 247 (4) (1958) 431–433.
[20] P. Vernotte, Les paradoxes de la theorie continue de l'equation de la chaleur, Comptes Rendus Hebd. Seances Acad. Sci. 246 (22) (1958) 3154–3155.
[21] P. Vernotte, La veritable equation de la chaleur, Comptes Rendus Hebd. Seances Acad. Sci. 247 (23) (1958) 2103–2105.
[22] P. Vernotte, Some possible complications in the phenomena of thermal conduction, Comptes Rendus Hebd. Seances Acad. Sci. 252 (1961) 2190–2191.
[23] D.Y. Tzou, Macro-to-microscale Heat Transfer; the Lagging Behavior, Taylor & Francis, Washington, DC, 1997.
[24] D.Y. Tzou, Temperature-dependent thermal lagging in ultrafast laser heating, Int. J. Heat Mass Transfer 44 (2001) 1725–1734.
[25] P. Vadasz, Conditions for local thermal equilibrium in porous media conduction, Transport in Porous Media 59 (2005) 341–355.
[26] P. Vadasz, Absence of oscillations and resonance in porous media dual-phase-lagging Fourier heat conduction, ASME J. Heat Transfer 127 (2005), in press.
[27] P. Vadasz, J.J. Vadasz, S. Govender, Heat transfer enhancement in nanofluid suspensions, Proceedings of IMECE2004, Paper No. IMECE2004-59840, 2004.
[28] M.J. Assael, M. Dix, K. Gialou, L. Vozar, W.A. Wakeham, Application of the transient hot-wire technique to the measurement of the thermal conductivity of solids, Int. J. Thermophys. 23 (2002) 615–633.
[29] J.J. De Groot, J. Kestin, H. Sookiazian, Instrument to measure the thermal conductivity of gases, Physica 75 (1974) 454–482.
[30] J.J. Healy, J.J. de Groot, J. Kestin, The theory of the transient hot-wire method for measuring thermal conductivity, Physica 82C (1976) 392–408.
[31] J. Kestin, W.A. Wakeham, A contribution to the theory of the transient hot wire technique for thermal conductivity measurements, Physica 92A (1978) 102–116.
[32] U. Hammerschmidt, W. Sabuga, Transient hot wire (THW) method: Uncertainty assessment, Int. J. Thermophys. 21 (2000) 1255–1278.
[33] Y. Nagasaka, A. Nagashima, Absolute measurement of the thermal conductivity of electrically conducting liquids by the transient hot-wire method, J. Phys. E: Sci. Instrum. 14 (1981) 1435–1440.
[34] S.E. Gustafsson, Transient hot strip techniques for measuring thermal conductivity and thermal diffusivity, The Rigaku J. 4 (1987) 16–28.
[35] M.N. Özisik, D.Y. Tzou, On the wave theory in heat conduction, J. Heat Transfer 116 (1994) 526–535.
[36] A. Haji-Sheikh, W.J. Minkowycz, E.M. Sparrow, Certain anomalies in the analysis of hyperbolic heat conduction, J. Heat Transfer 124 (2002) 307–319.
[37] L. Wang, Solution structure of hyperbolic heat-conduction equation, Int. J. Heat Mass Transfer 43 (2000) 365–373.
[38] J.I. Frankel, B. Vick, M.N. Özisik, Flux formulation of hyperbolic heat conduction, J. Appl. Phys. 58 (1985) 3340–3345.
[39] B. Vick, M.N. Özisik, Growth and decay of a thermal pulse predicted by the hyperbolic heat conduction equation, J. Heat Transfer 105 (1983) 902–907.